



Journal of Advanced Research in Fluid Mechanics and Thermal Sciences

Journal homepage:

https://semarakilmu.com.my/journals/index.php/fluid_mechanics_thermal_sciences/index

ISSN: 2289-7879



Impact of Geometrical Parameters on Heat Transfer Characteristics of SiO₂-Water Nanofluid Flow through Rectangular Corrugated Channels

Elhadi Kh. Abugnah^{1,2,*}, Wan Saiful-Islam Wan Salim¹, Abdulhafid M Elfaghi^{1,3}

¹ Faculty of Mechanical and Manufacturing Engineering, Universiti Tun Hussein Onn Malaysia, 86400 Batu Pahat, Johor, Malaysia

² College of Engineering Technology Janzour, Libya

³ Faculty of Engineering, University of Zawia, Libya

ARTICLE INFO

Article history:

Received 16 December 2022

Received in revised form 3 March 2023

Accepted 12 March 2023

Available online 26 March 2023

Keywords:

Corrugated channels; nanofluids; heat transfer; pressure drop; CFD

ABSTRACT

Design and performance of thermal devices are improved by optimizing their geometrical parameters. This study utilized numerical simulation to examine the heat transfer and flow properties of a rectangular corrugated channel at which nanofluid of silicon dioxide (SiO₂) and water is flowing. It is determined how the height-to-width ratio (h_c/W) and pitch-to-length ratio (pch/L) of a structure affect its thermal and hydraulic properties. The numerical simulations of flow include nanofluids with SiO₂-to-water volume fractions of 8% is accomplished by employing the finite volume method (FVM) with SIMPLE algorithm for discretization of the governing equations and coupling of the pressure-velocity system while the $k-\epsilon$ turbulence model was employed to resolve turbulence. The results demonstrate that, in comparison to the (Pch/L) ratio, the (h_c/W) ratio has a stronger influence on the enhancement of heat transfer. In reference to the values at minimum Re ($Re = 10000$), the ratio $Pch/L = 0.05$ offers the largest increase in Nu_{av} over the Re range by 180.8%. At Reynolds number (Re) 30000, an increase in 99.5% of average Nusselt number (Nu_{av}) is obtained when the (h_c/W) ratio is increased from 0.0 to 0.05. The numerical results indicate that the h_c/W of 0.05 with a Pch/L of 0.1075 are the optimum parameters and have shown significant improvement in thermal performance criteria (PEC).

1. Introduction

Due to the urgent requirement to achieve great thermal performance while minimizing weight and cost, several sectors are searching for innovative techniques to boost heat transfer in heat exchange devices. In this regard, one particular technique for increasing thermal performance while lowering the thickness of the thermal boundary layer on heat exchanger surfaces is the introduction of corrugated surfaces. The main objective of this passive technique is to increase heat exchange between the fluid and the surface by creating a secondary flow close to the corrugation. Besides geometrical parameters, the use of novel heat exchange mediums such as nano-fluids is also introduced to further enhance heat transfer. Traditional convective fluids have restricted thermal

* Corresponding author.

E-mail address hd180040@siswa.uthm.edu.my

<https://doi.org/10.37934/arfmts.104.2.86102>

characteristics, especially in terms of thermal conductivity, which can be a significant barrier to attaining high thermal performance. Using nanofluids with superior thermal properties, as a heat transfer medium in such channels can improve the heat exchange process, resulting in improved heat exchanger thermal efficiency. Both numerical and experimental studies have been conducted to study the performance of corrugated channels as heat exchange devices with conventional fluids in their computational investigation of the flow field and heat transfer properties of a single-start spirally corrugated tube, Li *et al.*, [1] found that the spirally corrugated tube could perform heat transfer more effectively than a smooth (non-corrugated) tube. A similar study by Rainieri *et al.* [2,3] focuses on flow a high-viscosity fluid in a spirally corrugated tube and found that the heat transfer characteristic of a spirally corrugated tube was superior to that of a smooth tube, particularly at high Reynolds numbers (Re). Other numerical work includes evaluation of turbulence models used in CFD simulations for various geometries. In their computational investigation on turbulent flow in a channel across periodic square grooves, Eiamsa-ard, *et al.*, [4] used four different turbulence models. They discovered that the RNG and standard k- ϵ turbulence models have better agreements with available measurements data than other turbulence models. Finally, they found that the grooved channel improves heat transfer significantly. Ajeel *et al.*, [5] used a computational model to investigate the effects of nanofluid flow across two different trapezoidal channel configurations: symmetrical and zigzag. The results showed that in terms of thermal performance, the symmetry profile outperformed the zigzag profile, and that the silicon dioxide-water nanofluid had the best Performance Evaluation Criteria (PEC) rate. Muhammad Asif *et al.*, [6] used ANSYS CFX software in their study to analyze the thermal performance of the corrugated plate heat exchanger (PHE) in single-phase flow. The purpose of this study was to create a generalized Nusselt number correlation for two different chevron angle plates—30°/30° and 60°/60°—in a commercial plate heat exchanger PHE setup with single-phase flow. A steady state simulation was run for a Reynolds number range of 500 to 2500 while maintaining a Prandtl number range of 3.5 to 7.5. The findings demonstrated that increasing Reynolds number and increasing the chevron angle both enhance Nusselt number. The Prandtl number had a negligible impact on the Nusselt number, though. For flow beneath a corrugated heat exchanger with corrugation angles of 30, 40, and 50 degrees, the heat transfer coefficient and friction factor of water, water+SiO₂, are calculated by D.Anjibabu *et al.*, [7], laminar flow experiments are being conducted at a bulk temperature of 60 °C. The experimental data demonstrates that an increase in Reynolds number increases heat transfer coefficient, and the best results are obtained with a corrugation angle of 50 degrees since considerable turbulence is produced at moderate speeds. The effect of corrugation arrangement on the thermal, hydraulic, and overall energy performances of nanofluid flows in corrugated tubes was investigated by Amr Kaood [8]. A thoroughly validated computational fluid dynamics (CFD) model was used to investigate several fluids (distilled water "DW," GNP-SDBS/DW, Al₂O₃/DW, and SiO₂/DW) and tube geometries (rectangular, triangular, trapezoidal, and curved ribs). The largest overall performance improvement (around 37%) was found for GNP-SDBS/DW nanofluid flow in a curvedly ribbed tube at Re of 10,000 compared to DW flow in a smooth tube. With Reynolds values greater than 10,000, it was discovered that the overall performance improvement decreased for all fluids and tube geometries. Regardless of the fluid type, tubes with curved ribs function better at medium and high flow rates. Trapezoidal ribs can be employed to increase heat transfer rates, but, when pumping power consumption is not a key concern or when flow rates are modest. Veysel *et al.*, [9] showed that circular cross-sectional rings with varying spacing ratios for heat transfer augmentation resulted in an 18% overall improvement. Experimental research was done by Aliabad *et al.*, [10] on forced convective flows of various nanofluids via a corrugated wavy channel under a condition of constant wall temperature. Effects of several parameters, such as base fluid kinds, oxide nanoparticle types, and nanoparticle

concentration on various volumetric flow rates were studied. The findings show that for all flow rate values, the Nusselt number increases and the Fanning friction factor decreases as the concentration of copper nanoparticles changes. Furthermore, it is demonstrated that among the investigated oxide nanoparticles in deionized water, the SiO_2 - and CuO -deionized water nanofluids give the best thermal-hydraulic performances, respectively. Jin *et al.*, [11] looked into the impacts of Re , the geometrical characteristics of corrugation (pitch and corrugation depth) and other variables on heat transfer performance. The impacts of the mentioned variables on heat transfer performance were investigated using numerical methods and validated by experiments. The findings showed that the heat transfer coefficient h and the Nu progressively decrease as the pitch increases. The secondary flow velocity and the vorticity of the longitudinal vortex both increases with corrugation depth.

Ajeel *et al.*, [12,13] investigated the effects of geometrical factors on the performance of the system in terms of the performance evaluation criterion (PEC) in various corrugated channels. In the work, simulation results showed that the height-to-width ratio was more significant compared to the pitch-to-length ratio in terms of PEC (higher PEC). In addition, they studied the effect of nano-fluid mixture and found that different volume fractions together with Re alters the flow structures, thereby affecting heat transfer. In most existing studies, flow and heat transfer were assumed to be two-dimensional in nature. This may not be the case when the channel cross-sectional area is relatively small with the boundary layer developing on non-heated walls interfering with the bulk flow. The current work examines turbulent forced convective channel flow of SiO_2 -water nanofluid mixture with heated rectangular corrugated surfaces. This was done over the Re range between 10,000 to 30,000 range and the effects of different design parameters are explored. This range is selected due to the large applications of heat transfer systems which exposed to such work flows and due to the lack of studies which deals with this sort of flows in conjunction with this geometry. The objective of this paper is to evaluate the effects of channel geometrical parameters, namely the pitch-to-height and the width-to-height ratios, on the channel heat transfer performance. Heat transfer and pressure drop along the channel is represented by the Nusselt Number and pressure drop respectively. In addition, the performance evaluation criteria (PEC) are estimated to indicate how the relationship between the two parameters.

2. Geometrical Parameters of Corrugated Channel

Figure 1 shows the geometry of the corrugated channel used in this investigation. The channel is made up of three main parts: an upstream section, a corrugated section, and a downstream section. The upstream section is four times the length of the downstream section, whereas the total length of the corrugated wall is twice that of the downstream wall. The channel's height (H) is 10 mm, while its width (W) is $(5H)$. h_c and P_{ch} denotes the corrugated height and longitudinal pitch, respectively. The current study is carried out on a total of four channel geometries comprising one straight channel and three rectangular corrugated channels with varying geometrical properties as described in Table 1. A constant heat flux is applied to the surfaces (top and the bottom surfaces) of the corrugated sections with the remaining surfaces kept adiabatic.

Table 1
 Place Design criteria used in the present study

| Channel Geometrical Parameter | Symbol | Value |
|-------------------------------|------------|----------------------------------|
| Height | H | 10 mm |
| Sectional length | L | $4*W$ |
| Pitch to length ratio | P_{ch}/L | 0.0750, 0.0625, 0.050, 0.1075 |
| Height to width ratio | h_c/W | Non-corrugated, 0.05, 0.04, 0.03 |

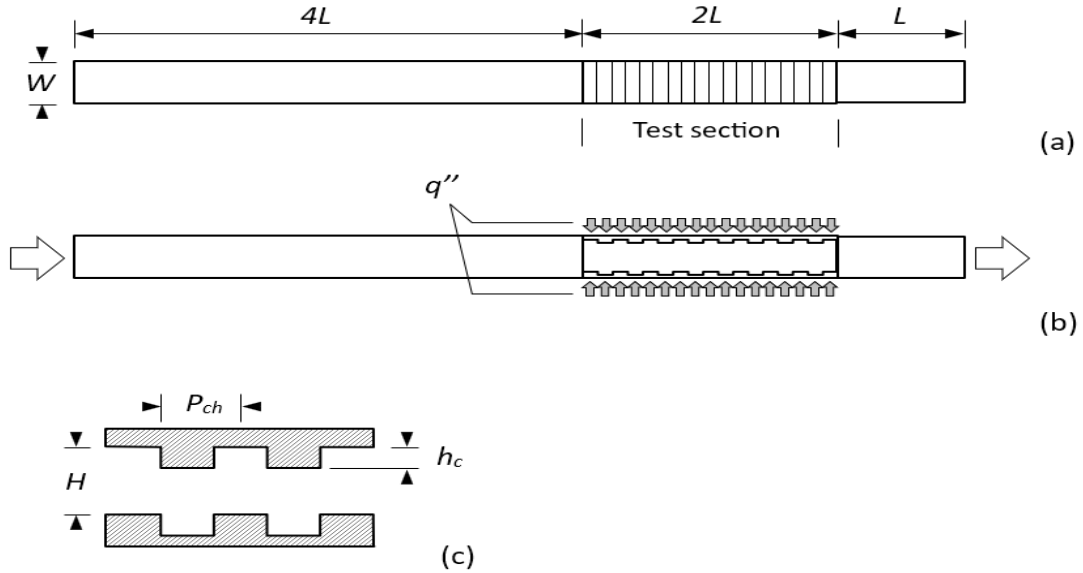


Fig. 1. Configuration of: (a) Computational domain, (b) Test section, (c) Corrugation geometry

3. Mathematical Model and Boundary Conditions

The Newtonian flow along the test section is assumed to be steady, incompressible, three-dimensional and fully developed. The governing conservation equations for mass, momentum and energy are shown below [14,15,25]

Continuity equation

$$\nabla \cdot (\rho_f V) = 0 \quad (1)$$

Momentum equation

$$\nabla \cdot (\rho_f VV) = -\nabla P + \nabla \cdot \tau \quad (2)$$

Energy equation

$$\nabla \cdot (\rho_f V C_{p,f}) = -\nabla \cdot (k_f \nabla T - C_{p,f} \rho_f \bar{v} t) \quad (3)$$

where V is dimensionless velocity vector, ∇P pressure gradient and ∇T temperature gradient, τ is wall shear stress, ρ_f is nanofluid density and C_p is specific heat at constant pressure. These equations

are solved with boundary conditions shown below, which are set at the inlet, exit and corresponding wall sections.

Inlet velocities are set at the inlet boundary with fluid temperature of 300K (Eq. (1)) while a pressure outlet boundary condition is set at the exit of the channel (Eq. (2)). A no-slip condition is imposed at every wall section (Eq. (3)). The corrugated surface of the channel is subjected to 10,000 W/m^2 while the remaining walls are set to be adiabatic.

Table 2
Summary of boundary conditions

| Boundary conditions | Hydraulic | Thermal | Kinetic energy | Turbulent dissipation rate |
|---------------------|---|-------------------|---------------------|--------------------------------|
| Inlet | $u=u_{in}, v=w=0$ | $T_{in}=300K$ | $K=k_{in}$ | $\varepsilon=\varepsilon_{in}$ |
| Outlet | $\frac{du}{dx} = \frac{dv}{dx} = \frac{dw}{dx} = 0$ | $\frac{dT}{dx}=0$ | $\frac{dk}{dx} = 0$ | $\frac{d\varepsilon}{dx} = 0$ |
| Wall | $u=v=w=0$ | $q=q_{wall}$ | - | - |

where u, v, w are velocity components along x, y, z directions, q is heat flux.

A two-equation turbulence model, namely the $k-\varepsilon$ is adopted in this simulation. The turbulent kinetic energy (k_{in}) and turbulent dissipation (ε_{in}) at the inlet are calculated using the turbulent intensity I using the following recommendations by Muhammad *et al.*, [16]

$$k_{in} = \frac{3}{2} (u_{in} I)^2 \quad (4)$$

$$\varepsilon_{in} = C_{\mu}^{3/4} \frac{k^{3/2}}{L} \quad (5)$$

where I is the turbulent intensity given by

$$I = \frac{u'}{U} = 0.16 Re^{-1/8} \% \quad (6)$$

where u' is the root-mean-square of the velocity fluctuations and U is the mean velocity.

The dimensionless numbers characterizing flow and heat transfer are Reynolds number (Re) and Nusselt number (Nu) respectively, which are defined as [13]

$$Re = \frac{\rho u D_h}{\mu} \quad (7)$$

$$Nu_{av} = \frac{h_{av} D_h}{k_f} \quad (8)$$

where ρ is density, μ is the dynamic viscosity, D_h is the hydraulic diameter, h_{av} is the mean heat transfer coefficient, and k_f is the fluid thermal conductivity [13].

$$h_{av} = q'' \cdot \frac{\ln\left(\frac{T_w - T_{m.in}}{T_w - T_{m.out}}\right)}{(T_w - T_{m.in}) - (T_w - T_{m.out})} \quad (9)$$

$$q'' = \dot{m} c_p (T_{m.in} - T_{m.out}) / A \quad (10)$$

where A is the corrugated section surface area and $T_{m,in}$, $T_{m,out}$ are the working media's average temperatures at the inlet and outlet. Additionally, based on the Reynolds number, the inlet velocity can be calculated as follows [13]

$$u_{in} = \frac{Re \cdot \mu}{\rho D_h} \quad (11)$$

Through the use of the cross-sectional area (A_{cross}) and the wetted perimeter (P_w), the hydraulic diameter in the corrugated section is computed. As Mohammed [17] stated

$$D_h = \frac{4A_{cross}}{P_w} \quad (12)$$

The pressure drop can also be calculated using the friction factor as given by [17]

$$\Delta p = f \frac{l_{corr} u_{in}^2}{2D_h} \quad (13)$$

where l_{corr} is the corrugated section length, f is friction factor, defined as follows [17]

$$f = 4c_f \quad (14)$$

with the Fanning friction factor (C_f) given as [16]

$$c_f = \frac{2\tau_s}{\rho u_{in}^2} \quad (15)$$

Finally, the Nusselt No. enhancement ratio (Nu_{er}) and thermal performance criteria (PEC) are used to compare the corrugated channel to non-corrugated channel [18]

$$Nu_{er} = \frac{Nu_{av}}{Nu_{av,0}} \quad (16)$$

$$PEC = \frac{Nu_{av}/Nu_{av,0}}{(f/f_0)^{1/3}} \quad (17)$$

4. Nanofluid Properties

The density, the specific heat and the viscosity of the nanofluid are given as [19-21,26]

$$\rho_{nf} = (1 - \phi)\rho_{bf} + \phi\rho_p \quad (18)$$

$$Cp_{nf} = (1 - \phi)Cp_{bf} + \phi Cp_p \quad (19)$$

$$\mu_{nf} = \mu_{bf} \frac{1}{(1+\phi)^{0.25}} \quad (20)$$

where Φ is volume fraction of nanoparticles, ρ_{bf} is base fluid density, ρ_p is nanoparticles density, Cp_{bf} is specific heat at constant pressure of base fluid and Cp_p is specific heat at constant pressure of nanoparticles.

An empirical correlation that considered Brownian motion was utilised to determine effective thermal conductivity, as shown below [22]

$$k_{eff} = k_{static} + k_{Brownian} \quad (21)$$

$$k_{static} = k_{bf} \left[\frac{(k_p + k_{bf}) - 2\Phi(k_{bf} - k_p)}{(k_p + 2k_{bf}) + (k_p - k_{bf})} \right] \quad (22)$$

$$k_{Brownian} = 5 \times 10^4 \beta \Phi \rho_{bf} Cp_{bf} \sqrt{\frac{KT}{\rho_p d_p}} f(T, \Phi) \quad (23)$$

where k_p and k_{bf} are particle and base fluid conductivity respectively, K is Boltzmann constant ($K = 1.3807 \times 10^{-23}$ J/K) and β is a factor which is a function of Φ and dependent on the type of nanoparticles, as shown in Table 3.

$$f(T, \Phi) = (2.8217 \times 10^{-2} \Phi + 3.917 \times 10^{-3}) \left(\frac{T}{T_0} \right) + (-3.0669 \times 10^{-2} \Phi - 3.391123 \times 10^{-3}) \quad (24)$$

Table 3

Place Nanofluid properties ($dp = 20$ nm and $\phi = 0.8$)

| β | Concentration % | Temperature(K) |
|----------------------------|---------------------------|-------------------------|
| $1.9526(100\phi) - 1.4594$ | $1\% \leq \phi \leq 10\%$ | $298K \leq T \leq 363K$ |

Thermophysical properties (Table 4) of nanofluid (Water + SiO_2) are derived using the previous empirical formulae from the literature [20]

Table 4

Place Nanofluid properties ($dp = 20$ nm and $\phi = 0.8$)

| Property | Unit | Value |
|---------------------------|----------|----------|
| Density, ρ | kg/m^3 | 1094.344 |
| Dynamic viscosity, μ | Ns/m^2 | 0.004795 |
| Thermal conductivity, k | $W/m.K$ | 0.643072 |
| Specific heat, Cp | $J/kg.K$ | 3622.483 |

5. Numerical Procedure

The governing equations with accompanying boundary conditions are discretized using the finite volume method in a commercial CFD program, ANSYS-FLUENT (V16.1). The SIMPLE algorithm is contrasted with three other types of algorithms by Han HZ *et al.*, [22] for similar flow conditions: SIMPLEIC, PISO, and COUPLED. All algorithms have the same accuracy, but the SIMPLE algorithm has the fastest convergence rate. Therefore, the velocity and pressure fields are coupled using the SIMPLE algorithm, and a 2nd order upwind scheme is used to handle the convective terms. The standard k-model in FLUENT is the most extensively used turbulence model because it strikes a balance between computational economy and level of sophistication. Its prevalence in industrial flow and heat transfer simulations can be attributed to its robustness, efficiency, and reasonable accuracy over a wide range of turbulent flows, therefore the standard k- ϵ turbulent model is used, with the

diffusion term in the momentum and energy equations approximated by 2nd order upwind. Residues of 10^{-5} are forest for convergence of the continuity, momentum, and turbulence equations, while residues of 10^{-8} are set for convergence of the energy equation. The correctness of numerical methods findings is largely determined by the optimum grid test. For this purpose, five groups of grid sizes are evaluated on the non-corrugated channel, with water+ SiO₂ as the working liquid, as shown in Figure 2. It is seen that Nu_{av} is constant beyond 251980 grid count, hence this grid size is chosen for simulations in this study.

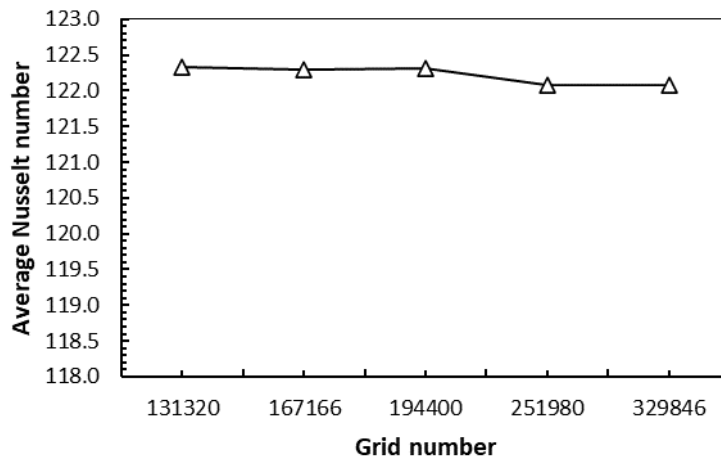


Fig. 2. Grid independence test

The empirical correlations of Pethukov *et al.*, [23] and Dittus-Boelter [24] are used to validate the friction factor and average Nusselt number. Figure 3 demonstrates that the numerical forecasts and the empirical correlations agree relatively well. When the Nu_{av} and f values for the current straight channel are compared to the standard correlations, they demonstrate good agreement with average relative error of 4% and 6%, respectively. The results of the corrugated channels were normalized using the straight channel's values.

$$\text{Pethukov} \quad f = (0.79 \ln(Re) - 1.64)^{-2} \quad (25)$$

$$\text{Dittus-Boelter} \quad Nu_{av} = 0.023 Re^{0.8} Pr^{0.4} \quad (26)$$

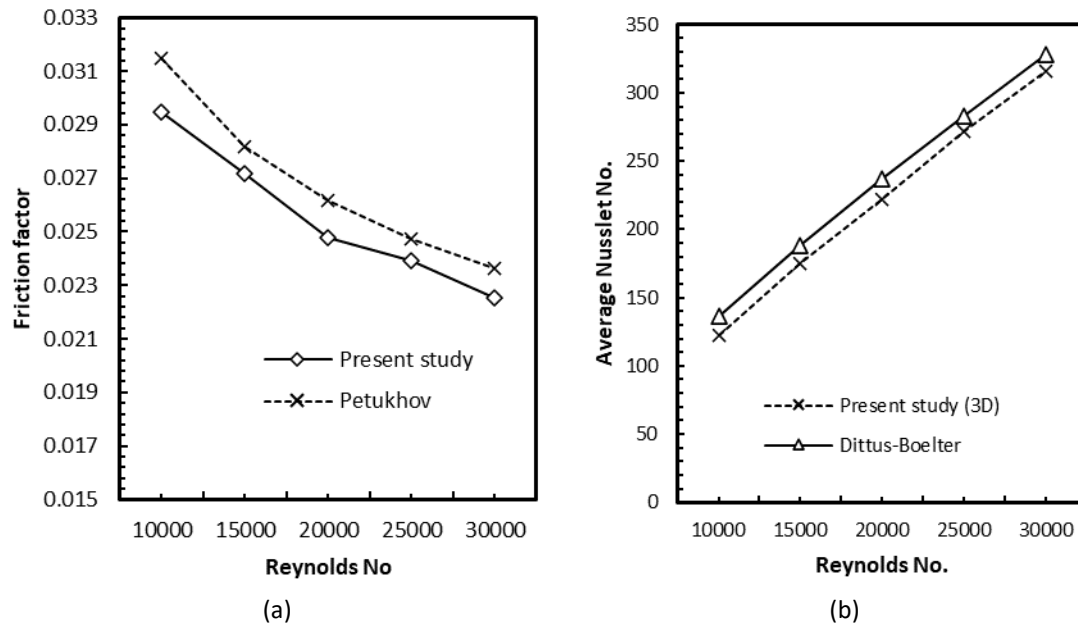


Fig. 3. Comparison between predicted (a) Friction factor (b) Average Nusselt number with the empirical correlations

6. Results and Discussions

In a rectangular-corrugation channel with Re ranges of 10,000–30,000 and volume fractions of 8%, numerical modelling of turbulent forced convection flow of SiO_2 -water nanofluid was conducted. Four distinct height-to-width ratios ($h/W = 0, 0.03, 0.04,$ and 0.05) and four different pitch-to-length ratios ($P_{ch}/L = 0.075, 0.0625, 0.05,$ and 0.1075) were taken into consideration in the current study.

6.1 Effect of Corrugation Pitch-to-Length ratio (P_{ch}/L) on Heat Transfer

The Nu_{av} and Nu_{er} variation with Re for various rectangular corrugation channel (P_{ch}/L) ratios are shown in Figure 4. Here, the ratio ($hc/W = 0.05$) is maintained while the ratio (P_{ch}/L) is examined for 0.075, 0.0625, 0.05 and 0.1075. For all P_{ch}/L scenarios investigated, the Nu_{av} linearly increases with the increase in Re . In reference to the values at minimum Re ($Re = 10000$), the ratio $P_{ch}/L = 0.05$ offers the largest increase in Nu_{av} over the Re range by 180.8%. This is followed by $P_{ch}/L = 0.0625$ (176.9% increase), $P_{ch}/L = 0.1075$ (172.1% increase) and $P_{ch}/L = 0.075$ (165.7% increase). On the other hand, it is the largest ratio $P_{ch}/L = 0.1075$ that offers the highest Nu_{av} among all cases investigated here ($Nu_{av} = 508.5$ at $Re = 30,000$) while the smallest ratio $P_{ch}/L = 0.05$ offers the lowest ($Nu_{av} = 401.2$ at $Re = 30,000$). At $Re = 30,000$, the channel ratio (P_{ch}/L) is increases from 0.05 to 0.1075, resulting in a 15 percent increase in Nu_{av} . The ratio of the Nu_{av} of SiO_2 -water nanofluid in the tested channel to the Nu_{av} of pure water in the flat channel with various P_{ch}/L ratios is shown in Figure 4(b). For all cases of P_{ch}/L , Nu_{er} increases as Re increases, with the biggest ratio P_{ch}/L providing the largest enhancement ratio.

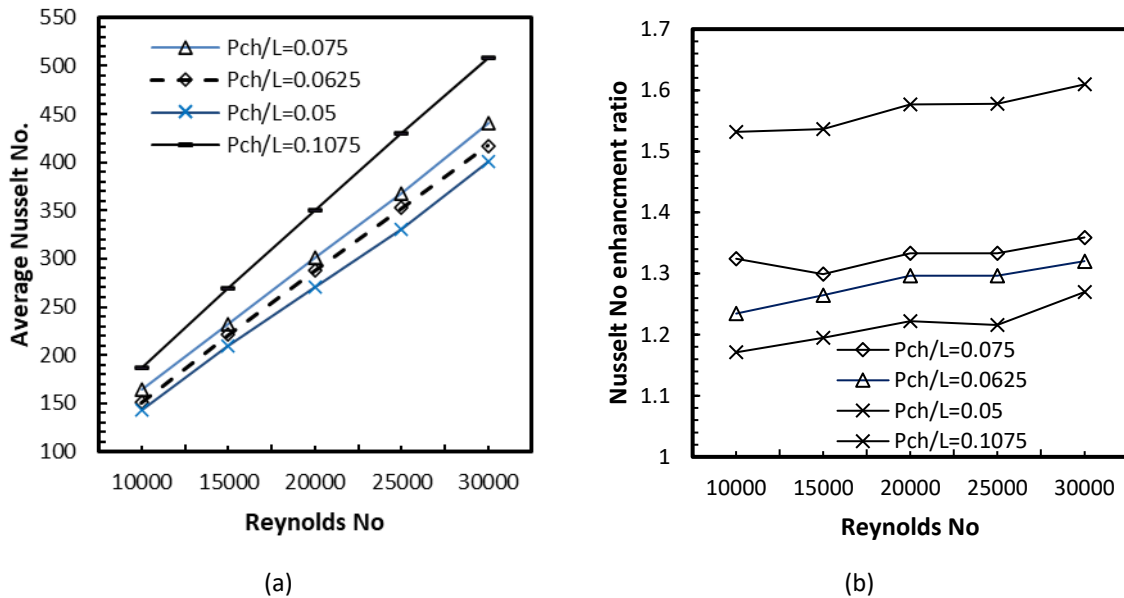


Fig. 4. The impact of various values of pitch to length ratio (P_{ch}/L) of rectangular- corrugation channel on (a) NU_{av} , (b) NU_{er}

Stronger turbulence is produced by the symmetry rectangular-corrugation channel with a larger P_{ch}/L ratio. Over the evaluated Re range, the rectangular-corrugation channel with highest ratio P_{ch}/L delivers the highest NU_{av} values. The velocity and temperature contours for these two cases are compared in Figure 5. It can be observed there that a larger recirculation zone is present in the case of $P_{ch}/L = 0.1075$, resulting in higher flow mixing and thereby increasing heat transfer, the velocity contours show substantial recirculation zones. On the lower surface, flow separations and recirculation take place at the cavity's border, but on the upper surface, the majority of flow separation takes place at the roof peaks and rear edges. The isotherm contours show the influence this has on the temperature contour. At the above-mentioned locations, bigger temperature change zones can be seen in channels with smaller pitch corrugations.

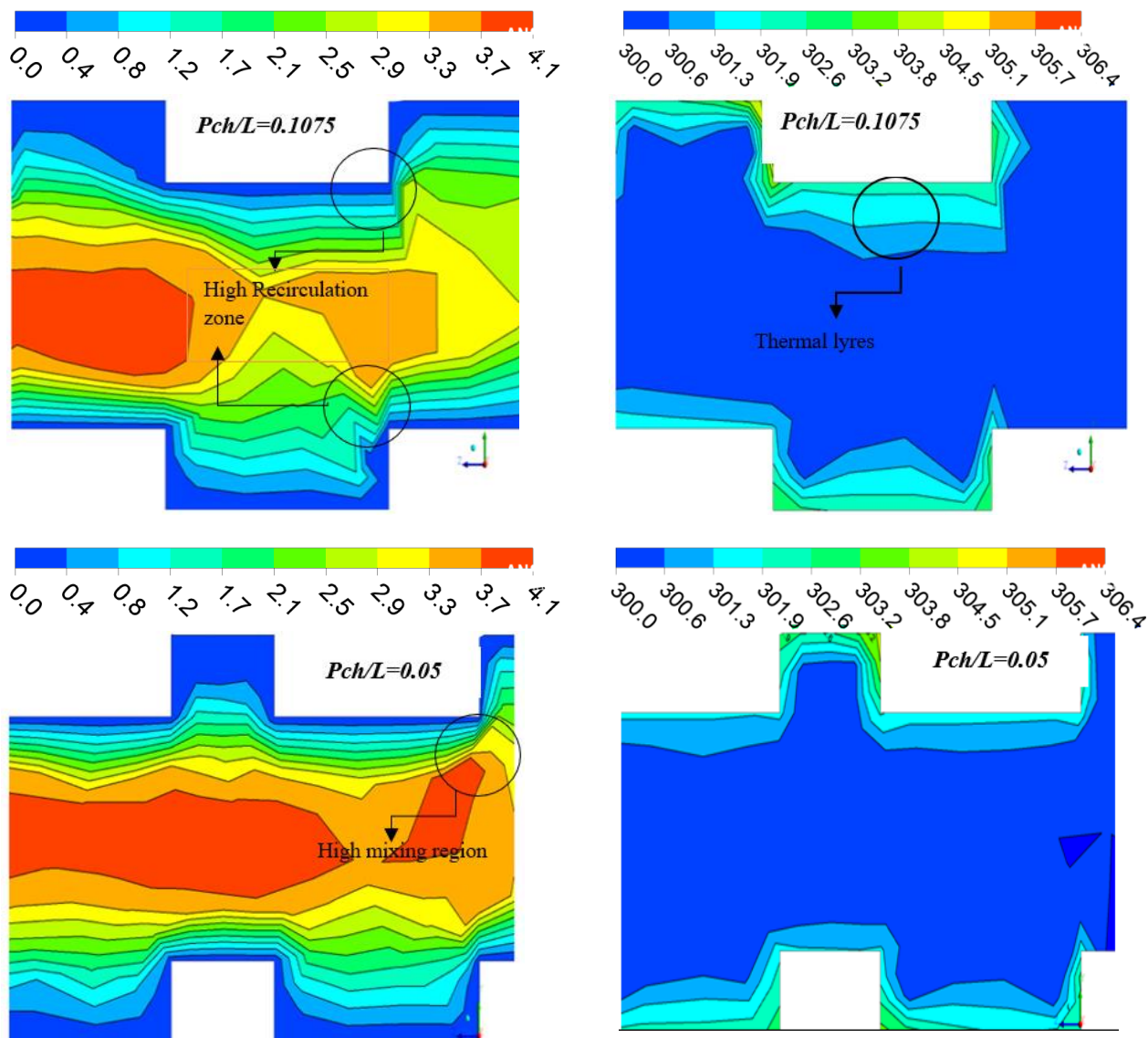


Fig. 5. Velocity and temperature contours for flow of SiO_2 -water nanofluids through rectangular – corrugation channel for largest and the lowest heat transfer enhancement corrugation ratio (P_{ch}/L)

6.2 Effect of Corrugation Pitch-to-Length ratio (P_{ch}/L) on Pressure Drop and PEC

In Figure 6(a), the influence of the corrugation ratio P_{ch}/L on pressure drop is demonstrated. For each value of the P_{ch}/L ratio, it's possible that Δp rises as Re rises. This reveals that the pressure loss will be greater in channels with a higher P_{ch}/L ratio. This has to do with how recirculation zones work, how the corrugated channel's flat length is changed, and how the longitudinal pitch is increased at the same Re .

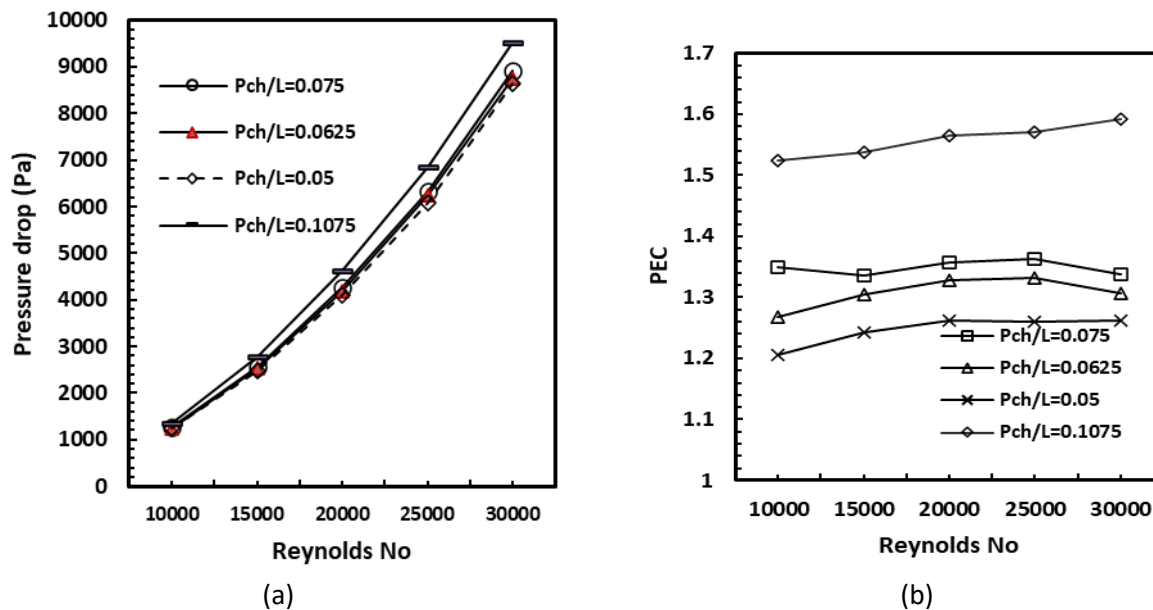


Fig. 6. The impact of various values of pitch to length ratio (P_{ch}/L) of rectangular- corrugation channel on (a) Pressure drop (b) PEC

The fluctuation of PEC versus Reynolds number with varies P_{ch}/L ratios for the channel under study is shown in Figure 6b. For all cases, the results reveal that PEC increases in lockstep with rising Re . For example, at Re between 10,000 and 30,000, PEC increases of 4.76 percent, 3.2 percent, -0.66, and 4.2 percent are seen for $P_{ch}/L = 0.05$, $P_{ch}/L = 0.0625$, $P_{ch}/L = 0.075$, and 0.1075 respectively. The PEC appears to be better at large P_{ch}/L ratios, with the maximum value being around 1.59 at $Re = 30,000$. It is possible that the largest P_{ch}/L ratio design provides the best PEC and fluid mixing for this particular corrugation geometry than the smallest P_{ch}/L arrangement shown.

6.3 The Effect of The Height to Width (h_c/W) Corrugation Ratio on Heat Transfer

The effects of various height to width ratios of the channel under study on the flow and heat fields have been assessed at the ideal value of P_{ch}/L ratio (0.1075) and $\phi = 8$ percent. The channel width (W) denotes the channel's width, whereas the corrugation height (h_c) denotes the corrugation's total height. The non-dimensional corrugation ratio (h_c/W) in this study ranges from 0.0 to 0.05. The Nu_{av} for various (h_c/W) ratios is shown in Figure 7(a). For all corrugation ratios of h_c/W , the Nu_{av} grows with Reynolds number. Furthermore, the Nu_{av} increases when the h_c/W ratio rises at a given Re . The development of the h_c/W ratio from 0.0 to 0.05 at $Re = 10,000$, which results in a 53% increase of Nu_{av} of that of non-corrugated channel and this improvement developed to reach 60% at $Re=30000$ which represented the peak value. At all Re values, the rectangular-corrugation channel with the largest ratio ($h_c/W = 0.05$) produces the highest Nu_{av} values.

Figure 7(b) shows the Nusselt number enhancement ratio for a channel with various height to width ratios. The figure clearly shows that adjusting the h_c/W ratio has a significant impact on the Nu_{er} . The influence of Re is slightly more dominating for higher height-to-width ratios, and the Nu_{er} is seen to be the same for all Re . Nu is enhanced at $Re=30000$ by 15.5 percent at $h_c/W = 0.05$, and it was the most enhancement ratio.

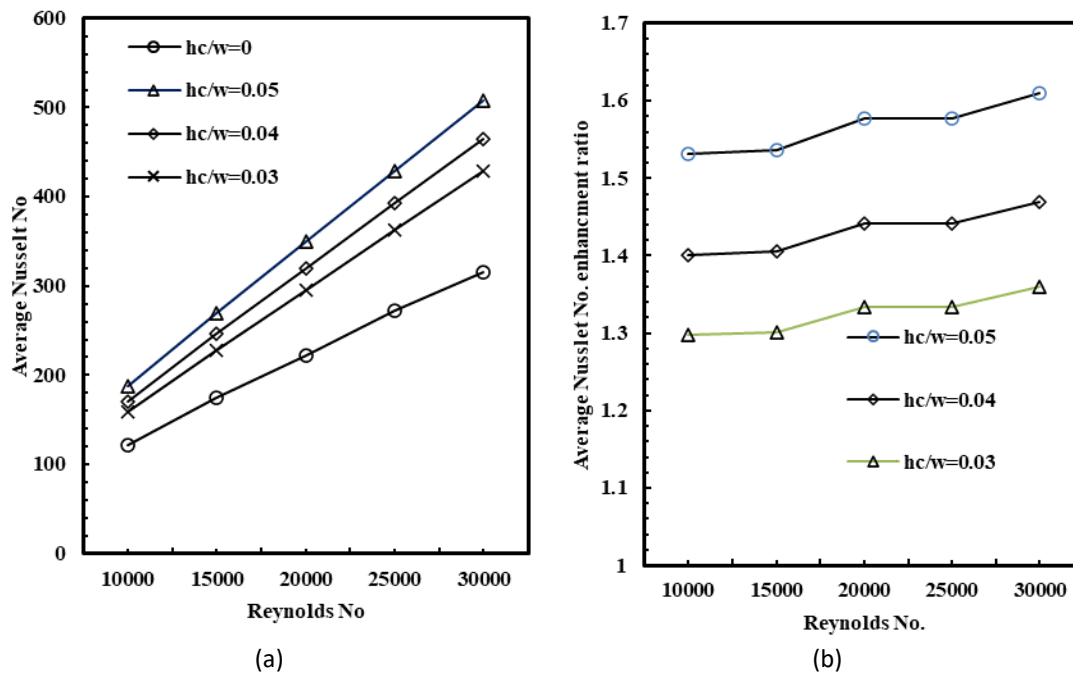


Fig. 7. The impact of height to width ratio (h_c/W) of rectangular corrugation channel on (a) Nu_{av} , (b) Nu_{er}

6.4 The Effect of The Height to Width (h_c/W) Corrugation Ratio on Pressure Drop and PEC

Figure 8(a) shows the pressure decrease as a function of Reynolds number for various h_c/W ratios. For all height to width selected ratios, the pressure drop increases with increasing Re. In comparison, the channel with a higher height to width ratio caused a significantly bigger pressure drop than the same channel with a lower h_c/W ratio especially at higher Nu about 14.9 percent. This might be explained by an increase in fluid velocity, which heightens shear stress along corrugated walls and raises the pressure as well as the intensity of recirculation zones to the main flow. As illustrated in Figure 9, for low h_c/W ratios, the presence of the corrugation has less of an impact on the main stream flow. Flow separation is also visible at the back half of each corrugation's bottom wall. The separating line continues toward the following corrugation when $h_c/W = 0.05$. In conclusion, the recirculation zones and fluid mixing are less in circumstances where $h_c/W = 0.04, 0.03$, compared to cases where $h_c/W = 0.05$, which also explains the previously discussed thermal characteristics.

The PEC is illustrated by Figure 8(b), as Re is increased, PEC is likewise shown to increase gradually. For example, at Reynolds numbers between 10,000 and 30,000, 4.26 percent, 4.36 percent, 4.65percent, increment in PEC are observed for $h_c/W = 0, 0.05, 0.04$, and 0.03 , respectively. As a result, for a given pressure drop, the symmetrical rectangular-corrugation channel with a high h_c/W (0.05) ratio can provide the best PEC with the largest heat transfer improvement, allowing for a more compact design for a given heat load.

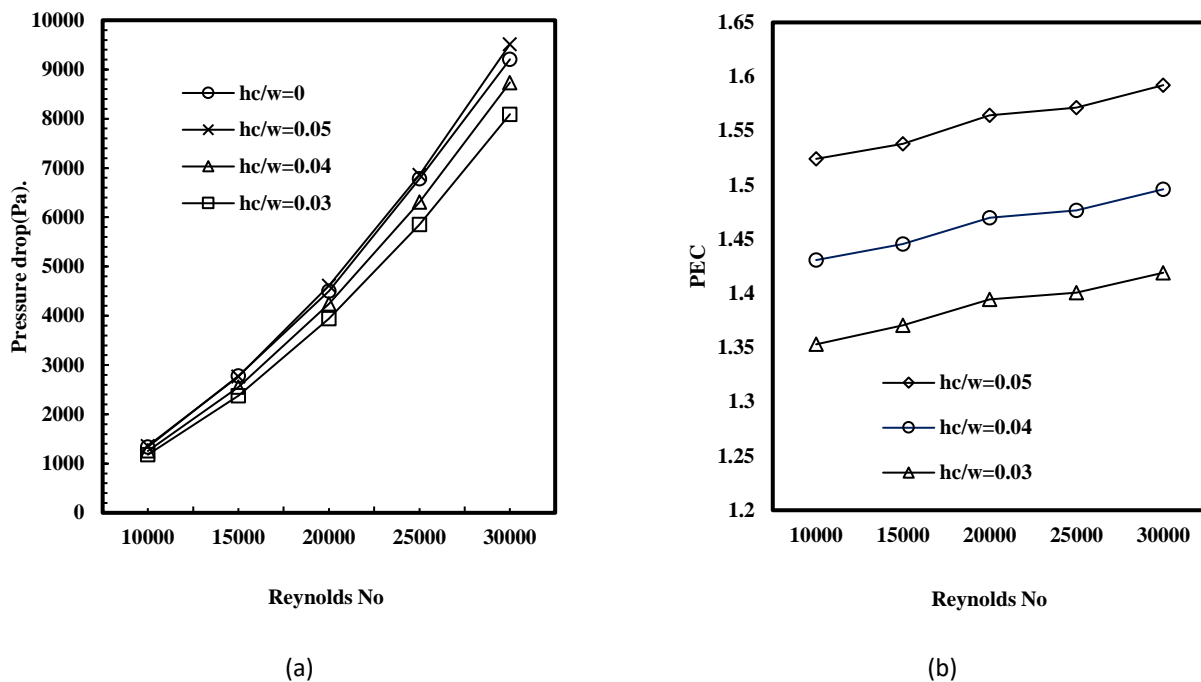


Fig. 8. The impact of height to width ratio (h_c/W) of rectangular corrugation channel on (a) ΔP , (b) PEC

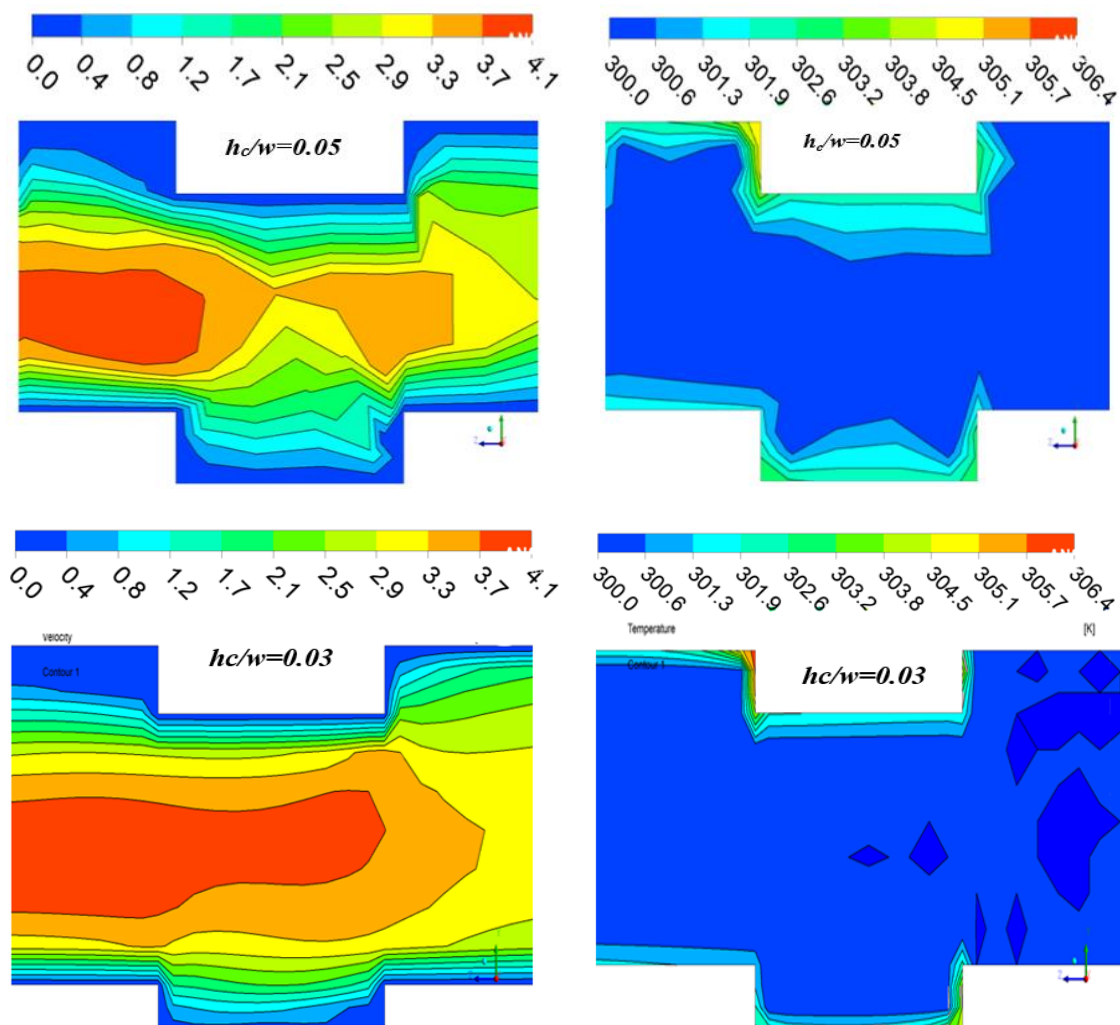


Fig. 9. Velocity and temperature contours for the flow SiO_2 -water nanofluid through rectangular corrugation channel for different corrugation ratio (h_c/W)

7. Conclusions

In the current work, turbulent flow of SiO₂-water nanofluid in a rectangular corrugation channel was computationally examined using the finite volume method. With a nanoparticle volume fraction of 0.08, the five Reynolds number varies from 10,000 to 30,000. The average Nusselt number, pressure drop, enhancement ratio, and thermal performance factor of the tested channel are displayed and examined in relation to Reynolds number, pitch to length ratio, and height to width ratio. The following are the study's main findings

- i. The results show that when the Reynolds number and corrugated height to width ratio of the tested channel increase, the average Nusselt number improves, but the pressure drop increases as well.
- ii. Additionally, as the pitch to length ratio of the corrugated channel increases, the average Nusselt number increases, resulting in a slightly pressure increment.
- iii. The h_c/W ratio has a bigger influence on thermal performance than the P_{ch}/L ratio.
- iv. For $h_c/W = 0.03, 0.04, \text{ and } 0.05$, respectively, increases in PEC of 4.26 percent, 4.36 percent, and 4.65 percent are seen at Reynolds numbers between 10,000 and 30,000.
- v. The h_c/W ratio of 0.05 and the corrugation ratio P_{ch}/L of 0.1075 are the best among the design variables examined, and they have a big influence on the PEC .

Finally, the current study can be recommended as a useful reference for designing more compact heat exchangers with high thermal efficiency.

Acknowledgement

The communication of this research is made possible through monetary assistance from the University Tun Hussein Onn Malaysia and the UTHM Publisher's Office through the Publication Fund E15216.

References

- [1] Li, Yaxia, Jianhua Wu, Hang Wang, Li-ping Kou and Xiaotao Tian. "Fluid Flow and Heat Transfer Characteristics in Helical Tubes Cooperating with Spiral Corrugation." *Energy Procedia* 17 (2012): 791-800. <https://doi.org/10.1016/j.egypro.2012.02.172>
- [2] Rainieri, Sara, Fabio Bozzoli and Giorgio Pagliarini. "Experimental investigation on the convective heat transfer in straight and coiled corrugated tubes for highly viscous fluids: Preliminary results." *International Journal of Heat and Mass Transfer* 55 (2012): 498-504. <https://doi.org/10.1016/j.ijheatmasstransfer.2011.08.030>
- [3] Rainieri, Sara, Fabio Bozzoli, Luca Cattani and Giorgio Pagliarini. "Experimental investigation on the convective heat transfer enhancement for highly viscous fluids in helical coiled corrugated tubes." *Journal of Physics: Conference Series* 395 (2012): 012032. <https://doi.org/10.1088/1742-6596/395/1/012032>
- [4] Eiamsa-ard, Smith and Pongjet Promvonge. "Numerical study on heat transfer of turbulent channel flow over periodic grooves." *International Communications in Heat and Mass Transfer* 35 (2008): 844-852. <https://doi.org/10.1016/j.icheatmasstransfer.2008.03.008>
- [5] Ajeel, Raheem K., W.S-I. W. Salim and Khalid bin Hasnan. "Thermal and hydraulic characteristics of turbulent nanofluids flow in trapezoidal-corrugated channel: Symmetry and zigzag shaped." *Case Studies in Thermal Engineering* (2018): 620–635. <https://doi.org/10.1016/j.csite.2018.08.002>
- [6] Asif, Muhammad, H. Aftab, H. A. Syed, M. A. Ali, and P. M. Muizz. "Simulation of corrugated plate heat exchanger for heat and flow analysis." *International Journal of Heat and Technology* 35, no. 1 (2017): 205-210. <https://doi.org/10.18280/ijht.350127>
- [7] Anjibabu, D., and Shaik Nayeem. "Heat transfer phenomenon of fluids in corrugated plate heat exchangers." *Int. J. Eng. Adv. Technol.* 8, no. 5 (2019): 2249-8958.

- [8] Kaood, Amr, and Muhammed A. Hassan. "Thermo-hydraulic performance of nanofluids flow in various internally corrugated tubes." *Chemical Engineering and Processing-Process Intensification* 154 (2020): 108043. <https://doi.org/10.1016/j.cep.2020.108043>
- [9] Ozceyhan, Veysel, Sibel Gunes, Orhan Buyukalaca, and Necdet Altuntop. "Heat transfer enhancement in a tube using circular cross sectional rings separated from wall." *Applied energy* 85, no. 10 (2008): 988-1001. <https://doi.org/10.1016/j.apenergy.2008.02.007>
- [10] Khoshvaght-Aliabadi, M., A. Zamzamin, and F. Hormozi. "Wavy channel and different nanofluids effects on performance of plate-fin heat exchangers." *Journal of Thermophysics and Heat Transfer* 28, no. 3 (2014): 474-484. <https://doi.org/10.2514/1.T4209>
- [11] Jin, Zhi-jiang, Fu-qiang Chen, Zhi-xin Gao, Xiao-fei Gao, and Jin-yuan Qian. "Effects of pitch and corrugation depth on heat transfer characteristics in six-start spirally corrugated tube." *International Journal of Heat and Mass Transfer* 108 (2017): 1011-1025. <https://doi.org/10.1016/j.ijheatmasstransfer.2016.12.091>
- [12] Ajeel, Raheem Kadhim, Wan Saiful-Islam Wan Salim, and Khalid Hasnan. "Heat transfer enhancement in semicircle corrugated channel: effect of geometrical parameters and nanofluid." *Journal of Advanced Research in Fluid Mechanics and Thermal Sciences* 53, no. 1 (2019): 82-94.
- [13] Ajeel, Raheem K., Wan Saiful-Islam Wan Salim and Khalid bin Hasnan. "Influences of geometrical parameters on the heat transfer characteristics through symmetry trapezoidal-corrugated channel using SiO₂-water nanofluid." *International Communications in Heat and Mass Transfer* 1 (101) (2019): 1–9. <https://doi.org/10.1016/j.icheatmasstransfer.2018.12.016>
- [14] Moraveji, Mostafa Keshavarz, Mehdi Darabi, Seyyed Mohammad Hossein Haddad and Reza Davarnejad. "Modeling of convective heat transfer of a nanofluid in the developing region of tube flow with computational fluid dynamics." *International Communications in Heat and Mass Transfer* 38 (2011): 1291-1295. <https://doi.org/10.1016/j.icheatmasstransfer.2011.06.011>
- [15] Yang, Yue-Tzu, Hsiang-Wen Tang, Bo-Yan Zeng and Chao-Han Wu. "Numerical simulation and optimization of turbulent nanofluids in a three-dimensional rectangular rib-grooved channel." *International Communications in Heat and Mass Transfer* 66 (2015): 71-79. <https://doi.org/10.1016/j.icheatmasstransfer.2015.05.022>
- [16] Mohammed, Hussein A., Azher M. Abed and Mazlan Abd. Wahid. "The effects of geometrical parameters of a corrugated channel with in out-of-phase arrangement." *International Communications in Heat and Mass Transfer* 40 (2013): 47-57. <https://doi.org/10.1016/j.icheatmasstransfer.2012.10.022>
- [17] Ahmed, M. A., Norshah Hafeez Shuaib, Mohd. Zamri Yusoff and Amir Al-Falahi. "Numerical investigations of flow and heat transfer enhancement in a corrugated channel using nanofluid." *International Communications in Heat and Mass Transfer* 38 (2011): 1368-1375. <https://doi.org/10.1016/j.icheatmasstransfer.2011.08.013>
- [18] Manca, Oronzio, Sergio Nardini and Daniele Ricci. "A numerical study of nanofluid forced convection in ribbed channels." *Applied Thermal Engineering* 37 (2012): 280-292. <https://doi.org/10.1016/j.applthermaleng.2011.11.030>
- [19] Santra, Apurba Kumar, Swarnendu Sen and Niladri Chakraborty. "Study of heat transfer due to laminar flow of copper–water nanofluid through two isothermally heated parallel plates." *International Journal of Thermal Sciences* 48 (2009): 391-400. <https://doi.org/10.1016/j.ijthermalsci.2008.10.004>
- [20] Wang, Xiangrong and Arun Sadashiv Mujumdar. "A review on nanofluids - part I: theoretical and numerical investigations." *Brazilian Journal of Chemical Engineering* 25 (2008): 613-630. <https://doi.org/10.1590/S0104-66322008000400001>
- [21] Abugnah, Elhadi Kh, Wan Saiful-Islam Wan Salim, Abdulhafid M. Elfaghi, and Zamani Ngali. "Comparison of 2D and 3D Modelling Applied to Single Phase Flow of Nanofluid through Corrugated Channels." *CFD Letters* 14, no. 1 (2022): 128-139. <https://doi.org/10.37934/cfdl.14.1.128139>
- [22] Vajjha, Ravikanth S., Debendra K. Das, and Devdatta P. Kulkarni. "Development of new correlations for convective heat transfer and friction factor in turbulent regime for nanofluids." *International journal of heat and mass transfer* 53, no. 21-22 (2010): 4607-4618. <https://doi.org/10.1016/j.ijheatmasstransfer.2010.06.032>
- [23] Han, Huai-Zhi, Bing-Xi Li, Hao Wu, and Wei Shao. "Multi-objective shape optimization of double pipe heat exchanger with inner corrugated tube using RSM method." *International Journal of Thermal Sciences* 90 (2015): 173-186. <https://doi.org/10.1016/j.ijthermalsci.2014.12.010>
- [24] Akbari, Omid Ali, Davood Toghraie, and Arash Karimipour. "Numerical simulation of heat transfer and turbulent flow of water nanofluids copper oxide in rectangular microchannel with semi-attached rib." *Advances in Mechanical Engineering* 8, no. 4 (2016): 1687814016641016. <https://doi.org/10.1177/1687814016641016>
- [25] Elfaghi, Abdulhafid MA, Alhadi A. Abosbaia, Munir FA Alkbir, and Abdoulhdi AB Omran. "CFD Simulation of Forced Convection Heat Transfer Enhancement in Pipe Using Al₂O₃/Water Nanofluid." *Journal of Advanced Research in Numerical Heat Transfer* 8, no. 1 (2022): 44-49. <https://doi.org/10.37934/cfdl.14.9.118124>

- [26] Rusdi, Nadia Diana Mohd, Siti Suzilliana Putri Mohamed Isa, Norihan Md Arifin, and Norfifah Bachok. "Thermal Radiation in Nanofluid Penetrable Flow Bounded with Partial Slip Condition." *CFD Letters* 13, no. 8 (2021): 32-44. <https://doi.org/10.37934/cfdl.13.8.3244>